ANTHROPOLOGY

Calcium isotopic patterns in enamel reflect different nursing behaviors among South African early hominins

Théo Tacail[1,2]*, Jeremy E. Martin[1]*, Florent Arnaud-Godet[1], J. Francis Thackeray[3], Thure E. Cerling[4], José Braga[3,5], Vincent Balter[1]†

Nursing is pivotal in the social and biological evolution of hominins, but to date, early-life behavior among hominin lineages is a matter of debate. The calcium isotopic compositions ($\delta^{44/42}$Ca) of tooth enamel can provide dietary information on this period. Here, we measure the $\delta^{44/42}$Ca values in spatially located microsized regions in tooth enamel of 37 South African hominins to reconstruct early-life dietary-specific variability in *Australopithecus africanus*, *Paranthropus robustus*, and early *Homo*. Very low $\delta^{44/42}$Ca values (<−1.4‰), indicative of milk consumption, are measured in early *Homo* but not in *A. africanus* and *P. robustus*. In these latter taxa, transitional or adult nonmilk foods must have been provided in substantial quantities relative to breast milk rapidly after birth. The results suggest that early *Homo* have continued a predominantly breast milk–based nursing period for longer than *A. africanus* and *P. robustus* and have consequently more prolonged interbirth interval.

INTRODUCTION

Inferring nursing behavior from the fossil record is a difficult task and has been based on body size determination, dental development, and geochemical analysis (1–8). High-resolution elemental analysis in dental tissues can provide information on early-life diet. Using laser ablation, Austin *et al.* (8) have shown that variations of the barium/calcium ratios (Ba/Ca) in human and macaque tooth enamel reflect breastfeeding and its decline with time. Recently, Tacail *et al.* (4) demonstrated that the $\delta^{44/42}$Ca values in deciduous tooth enamel of infants with known dietary histories during childhood vary according to the age of cessation of suckling. In both cases (4, 8), teeth were cut to locate incremental microstructure, notably the neonatal line, which serves as the starting point for age determination. While this approach is relevant to assess the dental microstructural calendar, it is not compatible with a large-scale study of rare museum fossil specimens such as hominins. Here, we spatially microsampled tooth enamel in a large set of South African hominins. We analyzed teeth of 12 specimens of *Australopithecus africanus*, 18 of *Paranthropus robustus*, and 7 of early *Homo*, representing a total of 84 enamel samples (*A. africanus*, $n = 28$; *P. robustus*, $n = 37$; early *Homo*, $n = 18$; see Materials and table S1). We also analyzed teeth of coexisting mammals including 7 specimens of browsers, 10 of grazers, and 7 of carnivores, as well as 4 modern teeth of *Gorilla gorilla gorilla* for comparison (Materials and table S1).

RESULTS

We report high-precision Ca isotopic values along with strontium/calcium (Sr/Ca) and barium/calcium (Ba/Ca) ratios (Methods and table S1). Fractionation between $\delta^{44/42}$Ca and $\delta^{43/42}$Ca is mass dependent (fig. S1), conforming to the expected mass-dependent fractionation slope of ~0.5 (9); hence, only $\delta^{44/42}$Ca is discussed here. Several trace elements (10, 11) and isotopic ratio (12, 13) patterns in the South Af-

rican Plio-Pleistocene fossil dental remains already proved that this material is extremely well preserved. For mass balance reasons, diagenesis is more sensitive for elements with a high water/rock ratio (14). Here, we monitored diagenesis using uranium and manganese and did not find any evidence of diagenesis for trace elements (Sr and Ba), which have a relatively high water/rock ratio, and all the more for Ca, which has the lowest possible water/rock ratio, being the most abundant element in hydroxylapatite (fig. S2).

DISCUSSION

The Ca isotopic compositions of dental enamel decrease with ascending trophic position in fish (15, 16), reptiles (17, 18), and mammals (19), and the Sr/Ba ratio recapitulates the Sr/Ca and Ba/Ca patterns, namely, that it slightly increases from grazers to browsers, and is much higher in carnivores (10, 11). Accordingly, here, carnivores have the lowest $\delta^{44/42}$Ca values (−1.75 ± 0.24, ±2 SD) and herbivores have the lowest Sr/Ba values (1.67 ± 1.14, ±2 SD) of the dataset (fig. S3). Between these two trophic end members, hominins occupy intermediate positions that are characterized by specific $\delta^{44/42}$Ca or Sr/Ba values (figs. S3 and S4, A and B). In this context, the contentious first molar KB5223 specimen, considered as early *Homo* by some authors (20) or as *P. robustus* by some others (21), falls within the domain of *P. robustus* (fig. S3). Together, the present results suggest that *P. robustus* consumed more plant-based foods than *A. africanus* and early *Homo* (11). In contrast with previous studies involving faunal assemblages, the South African hominin $\delta^{44/42}$Ca values alone cannot be interpreted in terms of trophic position. The $\delta^{44/42}$Ca values on late-forming teeth, i.e., second and third molars (fig. S4B), are similar for the three hominins, which apparently contradicts dietary interpretations. A review of literature data on various foodstuff $\delta^{44/42}$Ca values shows that meat does not differ isotopically from vegetal foodstuffs (fig. S5). A reconciling explanation is that trophic relationship using the Ca isotopic compositions is at work only when the skeleton of the prey is wholly or at least partly ingested with edible parts (17). Since hominins were unlikely to have consumed bone when they ate meat, this may explain why early *Homo* adults have similar $\delta^{44/42}$Ca values to *P. robustus* and *A. africanus*.

The notable lower average $\delta^{44/42}$Ca value of early *Homo* compared to the two other taxa is due to the fact that the deciduous second molar,
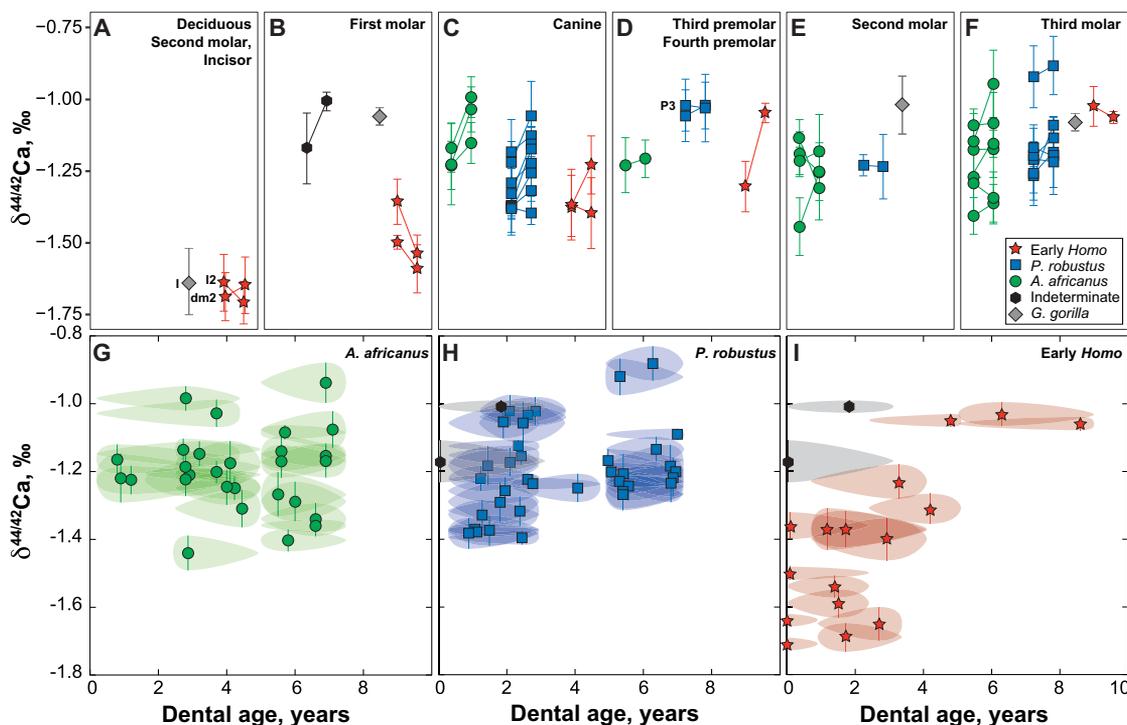
Fig. 1. Intraindividual and interindividual variability of tooth enamel $\delta^{44/42}$Ca values in modern and fossil hominins. (A to F) Distribution of the enamel $\delta^{44/42}$Ca values according to tooth types. The two microsampling spots processed in each tooth are linked, the "upper" spot being on the left side and the "lower" spot on the right. Error bars are two SDs of the mean. **(G to I)** Distribution of the enamel $\delta^{44/42}$Ca values according to reconstructed dental age. See Methods, table S2, and Supplementary Data for explanations on the dental age reconstruction. Error bars are 1 SD of the mean. Shadowed areas incorporate the uncertainties on the $\delta^{44/42}$Ca values and on the dental age.

incisor, first molar, and canine (Fig. 1, A to C) are ^{44}Ca depleted relatively to the other tooth types, i.e., third premolar and third molar (Fig. 1, D to F). In early *Homo*, there is a trend from very low $\delta^{44/42}$Ca values (~−1.7‰) in the deciduous second molar and second incisor to higher values in canines and, lastly, in the collar enamel of the fourth premolar (Fig. 1, A to D). This evolution roughly follows the mineralization calendar in *Homo* (*22, 23*). Unfortunately, this observation cannot be made for *P. robustus* and *A. africanus* because the sampling misses incisor and first molar. Although further investigation is necessary among extant primates, it is interesting to observe that one permanent incisor of a modern gorilla also exhibits a low $\delta^{44/42}$Ca value (~−1.6‰; Fig. 1A). Such a tooth type mineralizes early in the lifetime of gorillas (*24*). Permanent molars, which mineralize later, display $\delta^{44/42}$Ca values at ~−1‰ (Fig. 1, B, E, and F). Regarding trace element data, the enamel Sr/Ca ratio has been reported to increase (*25*) and the Ba/Ca ratio to decrease (*8*) with the introduction of solid foods. Therefore, the Sr/Ca and Ba/Ca ratios should show an increase and a decrease, respectively, from anterior to posterior teeth, which is not the case here. We do not observe any clear pattern between tooth types and the normalized Ca ratios (figs. S6, A to F, and S7, A to F).

To evaluate the influence of individual age on the $\delta^{44/42}$Ca values, we reconstructed a dental age timeline using the distance between microsampled points relative to enamel cervix and cusp tip (Methods, figs. S8 and S9, tables S2 and S3, and Supplementary Data) (*22, 23, 26–28*). After initial secretion, enamel continues to mineralize through the maturation process, which may blur the elemental and isotopic dietary history. Recently, Smith *et al.* (*29*) show that the Ba/Ca ratio cannot be overprinted for more than a month during enamel maturation. Given the typical

300-μm space resolution of the present microsampling approach, the maturation offset affecting the Ca isotope composition is likely to be nonsignificant.

Pairing $\delta^{44/42}$Ca values with dental ages allows distinguishing specific patterns of temporal evolution of the main hominin groups (Fig. 1, G to I). In *A. africanus*, there is no clear relationship between the $\delta^{44/42}$Ca value and dental age as the slope of the regression line is close to zero (0.003 ± 0.024, ±2 SE; R^2 = 0.002; P = 0.8100; fig. S10A). In *P. robustus*, there is a possible slight (0.017 ± 0.018, ±2 SE) but nonsignificant (R^2 = 0.088, P = 0.074) increase of the $\delta^{44/42}$Ca value with dental age (fig. S10B). By contrast, we observed a marked and significant increase in early *Homo*, the slope of the regression line between $\delta^{44/42}$Ca values and dental ages being 0.073 ± 0.031 (±2 SE; R^2 = 0.616; P = 0.0003; fig. S10C). These trends remain the same when the average dental ages and $\delta^{44/42}$Ca values for a given tooth are considered (fig. S10, D to F). The strong correlation between $\delta^{44/42}$Ca values and dental ages observed in early *Homo* and the existence of very low $\delta^{44/42}$Ca values (<−1.4‰) in the first years of life (Fig. 1I) suggest that early *Homo* infants have experienced a marked period of breastfeeding. Modern western human milk has a variable but very low $\delta^{44/42}$Ca value of −1.67 ± 0.37‰ (±2 SD) (*4, 30*). These low values are reflected in tooth enamel of human infants. The very low $\delta^{44/42}$Ca values in tooth enamel of breastfed infants (average of −1.91 ± 0.13‰, ±2 SD) drift toward more positive values after cessation of suckling (average of −1.58 ± 0.13‰, ±2 SD) (*4*). *P. robustus* and *A. africanus* do not exhibit these low $\delta^{44/42}$Ca values (Fig. 1, G and H), suggesting that infants of these two hominin taxa were breastfed with a lower intensity and/or frequency and a shorter duration

than those of early *Homo*. An early diet composed of solid adult food and sparse suckling bouts is eventually a parsimonious explanation to account for the Ca isotopic signatures of *P. robustus* and *A. africanus* infants. Such a type of early-life dietary behavior is compatible with that of extant wild great apes (Fig. 1, A, B, E, and F) (*31, 32*). But, positing that the milk of *P. robustus* and *A. africanus* mothers had such a $\delta^{44/42}$Ca value that could explain the enamel values of their infants is unlikely (table S4 and fig. S11). Here, again, the early-life evolution of the Sr/Ca and Ba/Ca ratios is poorly informative as no significant correlation is observed with dental age for any hominin taxon (figs. S6, G to I, and S7, G to I).

In conclusion, the breast milk–based nursing period has been longer for infants, and consequently, interbirth interval was more prolonged for mothers in the gracile lineage than in the robust one. Ca isotope compositions, associated with a microsampling approach that allows intratooth time resolution, offer unprecedented perspectives into the exploration of weaning behaviors during the evolution of hominid and, more generally, of mammals.

MATERIALS
Fossil samples
Sampling was performed on hominin and associated fauna tooth specimens curated at the Ditsong National Museum of Natural History (formerly the Transvaal Museum) in Pretoria, South Africa, and exported to France thanks to a SAHRA (South African Heritage Resources Agency) permit (ID 1484). The sampling of enamel was performed using the method described by Tacail *et al.* (*33*). Briefly, it consisted of drilling the enamel surface using a tungsten carbide drill mounted on a precise position drilling MicroMill device. Resulting holes were typically 350 to 400 µm wide and 200 to 300 µm deep. Accumulated powder on the rims of the holes was collected using razorblades and transferred to clean 7-ml Savillex vials. This procedure allowed ~60 to 80 µg of hydroxylapatite corresponding to about 22 to 30 µg of Ca to be recovered. Before each sampling, enamel surface, drill bits, and razorblades were washed using 99% pure ethanol and blown off using a compressed air duster.

Modern samples
To obtain some preliminary insights from a modern primate, Ca isotope variability in the western lowland gorilla, *G. gorilla gorilla*, was measured from tooth enamel powder of four individuals obtained in the course of a previous study (*34*). The samples originated from La Lopé National Park in Gabon and were obtained from the osteological collection of the Station d'Études des Gorilles et Chimpanzés under Autorisation de recherche du Centre National de la Recherche Scientifique et Technologique no.

AR0026/11/MENESSIC/CENAREST/CG/CST/CSAR and Autorisation d'entrée de l'Agence Nationale des Parcs Nationaux no. 000013/PR/ANPN/SE/CS/AEPN.

METHODS
Sample chemistry
The chemical processing of the samples was performed using the method described by Tacail *et al.* (*9*). Briefly, enamel samples were dissolved in 300 µl of suprapure 1 M HCl acid, of which 30 µl was saved for the determination of elemental concentrations, and the remaining 270 µl was processed through AG50X-W12 cation exchange

resin in 1 M HCl medium to dispose sample matrix. Ca and Sr fractions were collected in 6 M HCl medium. Ca fractions were then separated from Sr by loading samples onto columns filled with Sr-specific resin (Eichrom Sr-Spec) in suprapure 3 M HNO_3 medium. Blanks for the whole procedure did not exceed 100 ng of Ca (*9*).

Concentration measurements
Concentrations of Ca and Sr were measured on an inductively coupled plasma (ICP) atomic emission spectrometer (iCAP 6000 Series ICP, Thermo Fisher Scientific), and concentrations of Sr and Ba were measured on an inductively coupled plasma mass spectrometer (ICP-MS; 7500 CX, Agilent) following the procedure given by Balter and Lécuyer (*35*).

Isotopic measurements
Calcium isotope abundance ratios (^{44}Ca/^{42}Ca and ^{43}Ca/^{42}Ca) were measured using a multicollector ICP-MS (Neptune Plus, Thermo Fisher Scientific) following previously described methods (*9, 16, 18, 19, 33*). After purification, Ca samples were dissolved in ultrapure 0.05 M HNO_3, and Ca concentration was set at 1.5 ppm for all samples and standards. All Ca isotope compositions were expressed using the "delta" notation defined as follows for the ^{44}Ca/^{42}Ca ratio

$$\delta^{44/42}\text{Ca} = \left[\frac{(^{44}\text{Ca}/^{42}\text{Ca})_{\text{sample}}}{(^{44}\text{Ca}/^{42}\text{Ca})_{\text{ICP Ca Lyon}}} - 1 \right] \times 1000$$

where $(^{44}\text{Ca}/^{42}\text{Ca})_{\text{sample}}$ and $(^{44}\text{Ca}/^{42}\text{Ca})_{\text{ICP Ca Lyon}}$ are the Ca isotope abundance ratios measured in sample and ICP Ca Lyon reference standard, respectively. The ICP Ca Lyon standard, used as a bracketing standard, was a Specpure Ca plasma standard solution (Alfa Aesar) as previously described (*9, 16, 18, 19, 33*).

Dental age determination
Before and after sampling, a picture was taken for each tooth containing, when possible, the two microsampling holes. All the pictures were taken with the same magnification. The pictures were imported in Adobe Illustrator software. Several points were located on the pictures: (i) the cusp tip of the tooth crown (point A; fig. S8); (ii) the lowest point on the buccal or lingual enamel (point B; fig. S8); and (iii) the positions of the microsampling holes. The microsampling hole close to the cusp tip is annotated "upper" (point U) and that close to the cervix is annotated "lower" (point L; Tables S1 and S2 and fig. S8). Then, a line was drawn from A to B, following the long growth axis of the enamel. The positions of the points U and L microsampling holes were projected to that line, parallel to external incremental growth marks, when visible. The projected U and L positions on the AB line are marked U' and L'. Last, the distances from A to B (tooth height, t), from the points B to L' (a), and from the points B to U' (b) were measured in arbitrary units and reported on the picture. A complete list of the pictures showing these measurements is given in the Supplementary Data. The resulting relative positions (i.e., height of the projection of a microsampling hole relative to the tooth height, H%) were replaced in the chronology of dental development of early *Homo* (*22, 23, 26, 28*), *A. africanus* (*26, 27*), and *P. robustus* (*26, 27*). Dental development determination can be based on two different approaches: The first is based on synchrotron virtual imaging using counts of long-period (Retzius lines) and short-period (cross striations) internal incremental lines (*26*), and the second is based on counts of perikymata (*22, 23, 27, 28*). Using the charts provided in these references for a given taxon [early

Homo: Fig. 10.9 (*22*), Fig. 4 (*23*), Table G (*26*), Table 2 (*26*), and Tables 1 and 2 (*28*); *A. africanus* and *P. robustus*: Fig. 4 (*27*), Table G (*26*), and Table 2 (*26*)], the ages of dental development can be reconstructed independently. Both approaches yield similar results of crown initiation age and crown formation time for incisor, canine, premolar, first, and second molar (fig. S9).

Important uncertainties are associated with reconstructed dental ages for three main reasons. First, most of the teeth are worn, which precludes an accurate estimation of the original crown height. Second, for a given tooth type, the chronological age cusp tip must incorporate the time taken to form cuspal enamel to the initiation age. Third, the sampling spots were performed at a more or less constant depth, but this was not formally controlled and could lead to the sampling of varying amounts of enamel layers, notably of cuspal enamel. To integrate all these uncertainties and the variations of the two calendars of dental age, we therefore consider for each spot the youngest crown initiation age and the longest crown formation time specific of the tooth type. The minimum dental age (min) and maximum dental age (max) for each tooth are summarized in table S2. The relative positions of the microsampling holes were converted into dental age using the following equation

$$\text{Dental age} = \%H * \left[\frac{\text{max} - \text{min}}{100}\right] + \text{min}$$

The complete list of dental age calculations is given in table S3.

SUPPLEMENTARY MATERIALS

Supplementary material for this article is available at http://advances.sciencemag.org/cgi/content/full/5/8/eaax3250/DC1

Fig. S1. Three isotopes plot: $\delta^{43/42}$Ca (‰) as a function of $\delta^{44/42}$Ca (‰) relative to ICP Ca Lyon.
Fig. S2. Heat map of geochemical data.
Fig. S3. Distributions of the Sr/Ba ratios and $\delta^{44/42}$Ca values in the hominins and associated fossil fauna.
Fig. S4. Distributions Sr/Ba and $\delta^{44/42}$Ca values in late-forming teeth.
Fig. S5. Distributions of known or estimated isotope compositions of primary Ca dietary sources (‰) relative to ICP Ca Lyon.
Fig. S6. Intraindividual and interindividual variability of tooth enamel Sr/Ca values in fossil hominins.
Fig. S7. Intraindividual and interindividual variability of tooth enamel Ba/Ca values in fossil hominins.
Fig. S8. Diagram of the measurements for dental age reconstruction for a molar and an incisor.
Fig. S9. Comparison of enamel mineralization calendars in hominins.
Fig. S10. Correlation between age and $\delta^{44/42}$Ca values.
Fig. S11. Correlation between diet and milk $\delta^{44/42}$Ca values.
Table S1. Geochemical data (Sr/Ca, Ba/Ca, Sr, Ba, U, Mn, $\delta^{44/42}$Ca, and $\delta^{43/42}$Ca) of hominins, associated fauna, and modern gorilla.
Table S2. Chronology of dental development in hominins.
Table S3. Measurement data for hominin dental age determination.
Table S4. Compilation of diet and milk $\delta^{44/42}$Ca values available in the literature.
Supplementary Data

REFERENCES AND NOTES

1. P. C. Lee, Growth and investment in hominin life history evolution: Patterns, processes, and outcomes. *Int. J. Primatol.* **33**, 1309–1331 (2012).
2. M. A. Van Noordwijk, C. W. Kuzawa, C. P. Van Schaik, The evolution of the patterning of human lactation: A comparative perspective. *Evol. Anthropol.* **22**, 202–212 (2013).
3. L. T. Humphrey, Weaning behaviour in human evolution. *Semin. Cell Dev. Biol.* **21**, 453–461 (2010).
4. T. Tacail, B. Thivichon-Prince, J. E. Martin, C. Charles, L. Viriot, V. Balter, Assessing human weaning practices with calcium isotopes in tooth enamel. *Proc. Natl. Acad. Sci. U.S.A.* **114**, 6268–6273 (2017).
5. P. C. Lee, The meanings of weaning: Growth, lactation, and life history. *Evol. Anthropol.* **5**, 87–98 (1996).
6. J. M. DeSilva, A shift toward birthing relatively large infants early in human evolution. *Proc. Natl. Acad. Sci. U.S.A.* **108**, 1022–1027 (2011).
7. S. L. Robson, B. Wood, Hominin life history: Reconstruction and evolution. *J. Anat.* **212**, 394–425 (2008).
8. C. Austin, T. M. Smith, A. Bradman, K. Hinde, R. Joannes-Boyau, D. Bishop, D. J. Hare, P. Doble, B. Eskenazi, M. Arora, Barium distributions in teeth reveal early-life dietary transitions in primates. *Nature* **498**, 216–219 (2013).
9. T. Tacail, E. Albalat, P. Télouk, V. Balter, A simplified protocol for measurement of Ca isotopes in biological samples. *J. Anal. At. Spectrom* **29**, 529–535 (2014).
10. M. Sponheimer, J. A. Lee-Thorp, Enamel diagenesis at South African Australopith sites: Implications for paleoecological reconstruction with trace elements. *Geochim. Cosmochim. Acta* **70**, 1644–1654 (2006).
11. V. Balter, J. Braga, P. Télouk, F. Thackeray, Evidence for dietary change but not landscape use in South African early hominins. *Nature* **489**, 558–560 (2012).
12. V. Balter, J. Blichert-Toft, J. Braga, P. Télouk, F. Thackeray, F. Albarède, U–Pb dating of fossil enamel from the Swartkrans Pleistocene hominid site, South Africa. *Earth Planet. Sci. Lett.* **267**, 236–246 (2008).
13. M. Sponheimer, B. H. Passey, D. J. de Ruiter, D. Guatelli-Steinberg, T. E. Cerling, J. A. Lee-Thorp, Isotopic evidence for dietary variability in the early hominin *Paranthropus robustus*. *Science* **314**, 980–982 (2006).
14. J. E. Martin, T. Tacail, V. Balter, Non-traditional isotope perspectives in vertebrate palaeobiology. *Palaeontology* **60**, 485–502 (2017).
15. J. Skulan, D. J. DePaolo, Calcium isotope fractionation between soft and mineralized tissues as a monitor of calcium use in vertebrates. *Proc. Natl. Acad. Sci. U.S.A.* **96**, 13709–13713 (1999).
16. J. E. Martin, T. Tacail, S. Adnet, C. Girard, V. Balter, Calcium isotopes reveal the trophic position of extant and fossil elasmobranchs. *Chem. Geol.* **415**, 118–125 (2015).
17. A. Heuser, T. Tütken, N. Gussone, S. J. G. Galer, Calcium isotopes in fossil bones and teeth — Diagenetic versus biogenic origin. *Geochim. Cosmochim. Acta* **75**, 3419–3433 (2011).
18. J. E. Martin, P. Vincent, T. Tacail, F. Khaldoune, E. Jourani, N. Bardet, V. Balter, Calcium isotopic evidence for vulnerable marine ecosystem structure prior to the K/Pg extinction. *Curr. Biol.* **27**, 1641–1644.e2 (2017).
19. J. E. Martin, T. Tacail, T. E. Cerling, V. Balter, Calcium isotopes in enamel of modern and Plio-Pleistocene East African mammals. *Earth Planet. Sci. Lett.* **503**, 227–235 (2018).
20. J. Braga, J. F. Thackeray, Early *Homo* at Kromdraai B: Probabilistic and morphological analysis of the lower dentition. *C. R. Palevol.* **2**, 269–279 (2003).
21. R. S. Lacruz, Enamel microstructure of the hominid KB 5223 from Kromdraai, South Africa. *Am. J. Phys. Anthropol.* **132**, 175–182 (2007).
22. M. C. Dean, B. H. Smith, Growth and development of the Nariokotome Youth, KNM-WT 15000, in *The First Humans - Origin and Early Evolution of the Genus Homo*, F. E. Grine, J. G. Fleagle, R. E. Leakey, Eds. (Springer, 2009), pp. 101–120.
23. M. C. Dean, Measures of maturation in early fossil hominins: Events at the first transition from australopiths to early *Homo*. *Phil. Trans. R. Soc. Lond. B Biol. Sci.* **371**, 20150234 (2016).
24. M. C. Dean, B. A. Wood, Developing pongid dentition and its use for ageing individual crania in comparative cross-sectional growth studies. *Folia Primatol.* **36**, 111–127 (1981).
25. L. T. Humphrey, M. C. Dean, T. E. Jeffries, M. Penn, Unlocking evidence of early diet from tooth enamel. *Proc. Natl. Acad. Sci. U.S.A.* **105**, 6834–6839 (2008).
26. T. M. Smith, P. Tafforeau, A. Le Cabec, A. Bonnin, A. Houssaye, J. Pouech, J. Moggi-Cecchi, F. Manthi, C. Ward, M. Makaremi, C. G. Menter, Dental ontogeny in Pliocene and early Pleistocene hominins. *PLOS ONE* **10**, e0118118 (2015).
27. A. D. Beynon, M. C. Dean, Distinct dental development patterns in early fossil hominids. *Nature* **335**, 509–514 (1988).
28. D. J. Reid, D. Guatelli-Steinberg, Updating histological data on crown initiation and crown completion ages in southern Africans. *Am. J. Phys. Anthropol.* **162**, 817–829 (2017).
29. T. M. Smith, C. Austin, D. R. Green, R. Joannes-Boyau, S. Bailey, D. Dumitriu, S. Fallon, R. Grün, H. F. James, M.-H. Moncel, I. S. Williams, R. Wood, M. Arora, Wintertime stress, nursing, and lead exposure in Neanderthal children. *Sci. Adv.* **4**, eaau9483 (2018).
30. N.-C. Chu, G. M. Henderson, N. S. Belshaw, R. E. M. Hedges, Establishing the potential of Ca isotopes as proxy for consumption of dairy products. *Appl. Geochem.* **21**, 1656–1667 (2006).
31. J. van Lawick-Goodall, The behaviour of free-living chimpanzees in the Gombe Stream Reserve. *Anim. Behav. Monogr.* **1**, 161–311 (1968).
32. K. J. Stewart, Suckling and lactational anoestrus in wild gorillas (*Gorilla gorilla*). *J. Reprod. Fertil.* **83**, 627–634 (1988).
33. T. Tacail, P. Télouk, V. Balter, Precise analysis of calcium stable isotope variations in biological apatites using laser ablation MC-ICPMS. *J. Anal. At. Spectrom* **31**, 152–162 (2016).

34. J. E. Martin, D. Vance, V. Balter, Magnesium stable isotope ecology using mammal tooth enamel. *Proc. Natl. Acad. Sci. U.S.A.* **112**, 430–435 (2015).

35. V. Balter, C. Lécuyer, Determination of Sr and Ba partition coefficients between apatite and water from 5°C to 60°C: a potential new thermometer for aquatic paleoenvironments. *Geochim. Cosmochim. Acta* **68**, 423–432 (2004).

Citation: T. Tacail, J. E. Martin, F. Arnaud-Godet, J. F. Thackeray, T. E. Cerling, J. Braga, V. Balter, Calcium isotopic patterns in enamel reflect different nursing behaviors among South African early hominins. *Sci. Adv.* **5**, eaax3250 (2019).

Science Advances

Calcium isotopic patterns in enamel reflect different nursing behaviors among South African early hominins

Théo Tacail, Jeremy E. Martin, Florent Arnaud-Godet, J. Francis Thackeray, Thure E. Cerling, José Braga and Vincent Balter

ARTICLE TOOLS	http://advances.sciencemag.org/content/5/8/eaax3250
SUPPLEMENTARY MATERIALS	http://advances.sciencemag.org/content/suppl/2019/08/26/5.8.eaax3250.DC1
REFERENCES	This article cites 34 articles, 8 of which you can access for free http://advances.sciencemag.org/content/5/8/eaax3250#BIBL
PERMISSIONS	http://www.sciencemag.org/help/reprints-and-permissions

Use of this article is subject to the Terms of Service